INVERSION OF EDDY CURRENT SIGNALS IN A NONUNIFORM PROBE FIELD

F. Muennemann, B.A. Auld, C.M. Fortunko,[*] and S.A. Padget[*]

Edward L. Ginston Laboratory
Stanford University
Stanford, CA 94305

We present a simple analytical method for predicting the eddy current signal (ΔZ) produced by a surface flaw of known dimensions, when interrogated by a probe with *spatially* varying magnetic field. The model is easily parameterized, and we use it to construct inversion schemes which can extract overall flaw dimensions from multi-position, multifrequency measurements. Our method is a type of Born approximation, in which we assume that the probe's magnetic field at the mouth of the flaw can be used as a boundary condition on the electromagnetic field solutions inside the flaw. To simplify the calculation we have chosen a "rectangular" 3-dimensional flaw geometry for our model. We describe experimental measurements made with a new broadband probe on a variety of flaws. This probe operates in a frequency range of 200 kHz to 20 MHz and was designed to make the multi-frequency measurements necessary for inversion purposes. Since inversion requires knowledge of the probe's magnetic field shape, we describe experimental methods which determine the interrogating field geometry for any eddy current probe.

1. INTRODUCTION

Nondestructive testing by eddy currents has been in use for many decades. In this type of testing, the operator passes a probe with an oscillating magnetic field over the part to be tested, inducing surface eddy currents. A flaw in the surface interrupts the currents, changing the impedance of the probe, which the operator monitors on an oscilloscope. It is the change in impedance of the probe, ΔZ , that we call the eddy current signal.

[*] National Bureau of Standards, Fracture and Deformation Division, Boulder, CO 80302. Publications of NBS not copyrightable in U.S.A.

The problem of eddy current signal inversion can be roughly divided into two steps: the forward problem of predicting the signal produced by a given probe, flaw and display system, and the inverse problem of deducing the flaw parameters from the eddy current signals. In this paper, the only parameters in which we are interested are the flaw dimensions: length 2c, depth a, and opening Δu, as well as position.

As Fig. 1 suggests, we can make some gross deductions from the spatial extent of the eddy current response. When the crack is longer than the probe field distribution, the signal is observed over an extended distance of probe travel and the crack tips are identified by the points at which the signal disappears (eddy current imaging). A very small crack appears as a "point source" and gives a probe scan output signal whose shape is determined by the probe field (acting as a "window function") rather than the physical shape of the flaw. One can often recognize a non-crack feature by its spatial distribution.

When we attempt to invert eddy current signals from a large flaw, we are effectively dealing with a two-dimensional flaw, interrogated by a nonuniform field, except when the probe is near the tips of the flaw. Some general features of this problem are analyzed in reference 1 and we make a qualitative comparison with recent experimental results in the second part of the present paper. Since this is conceptually and physically a different problem than that of dealing with the very small flaws of interest to the aerospace industry (Retirement for Cause program), we will not discuss this case further here.

When the crack is smaller than the probe, the inversion problem becomes much more difficult. It is no longer possible to determine flaw length by "imaging" and the length 2c must be extracted, together with the other crack parameters a and Δu, from the data. Yet another problem we must deal with is crack positioning. When the crack is so small that the probe field determines the shape of the eddy current response, then the operator does not, in general, know where the crack is relative to the probe field. There is then a danger that inversion results will be incorrect since they will be based on an erroneous value of the probe field. Thus, a complete inversion procedure requires that we take the relative position of the crack to be an unknown parameter.

Because of the wide variation in testing conditions and materials, we develop a procedure in outline form, which we call an "inversion protocol". Our aim is to give general guidelines for inverting signals. However, each particular Non-Destructive Evaluation (NDE) application will require some modifications and allow some simplification by using *a priori* information. In many testing situations, for example, the aspect ratio a/c can be closely estimated from the stress gradient in the workpiece at the position of the crack so that the length 2c and the opening Δu suffice to define the crack
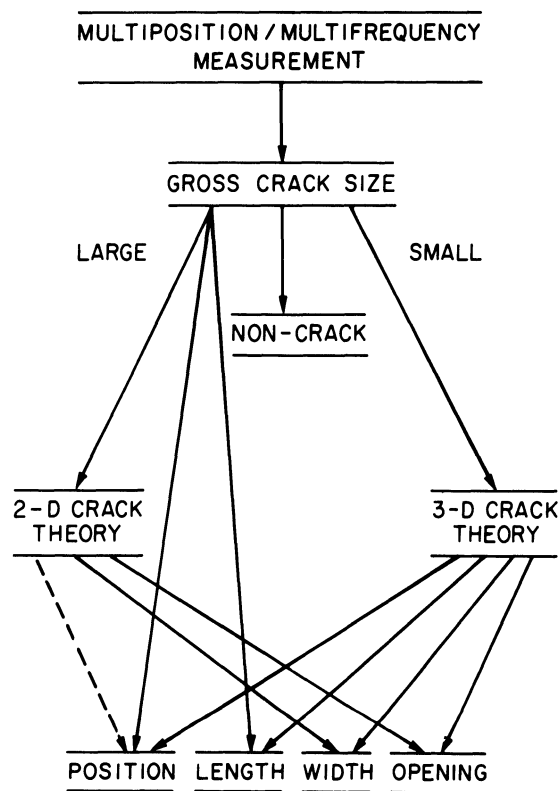
```
┌─────────────────────────────────────┐
│  MULTIPOSITION / MULTIFREQUENCY     │
│           MEASUREMENT               │
└─────────────────────────────────────┘
                  │
                  ▼
        ┌─────────────────────┐
        │  GROSS  CRACK  SIZE │
        └─────────────────────┘
   LARGE                    SMALL

            ┌───────────────┐
            │  NON-CRACK    │
            └───────────────┘

┌──────────────┐              ┌──────────────┐
│  2-D CRACK   │              │  3-D CRACK   │
│   THEORY     │              │   THEORY     │
└──────────────┘              └──────────────┘

┌──────────────────────────────────────┐
│ POSITION  LENGTH  WIDTH  OPENING     │
└──────────────────────────────────────┘
```

Fig. 1.   Overview of inversion protocol.

geometry. However, in view of the fact noted above, that the position
of the crack is a secondary unknown of the inversion problem, this
simplification is not always possible. We therefore develop a general
protocol and then simplify it for particular situations.

Our inversion strategy is determinate in that it supposes a crack
model with three parameters c, a , and Δu , and therefore requires
that we first solve the forward problem for the chosen model. We have
selected for this purpose a rectangular open flaw (Fig. 2) because
this is the only geometry for which a completely parameterized ana-
lytic solution is available. The forward and inverse problems are
treated in detail only for a/δ larger than unity, δ being the
electromagnetic skin depth. Studies to date[2,3,4] indicate that the
detection sensitivity is probably greatest in this region. However,
very recent experimental results for small a/δ show great promise,[4]
and signal inversion in this frequency range will also be briefly dis-
cussed. Using these results we propose a general inversion protocol
that extracts the position, length, depth, and opening of a crack from
multipositional and multifrequency eddy current measurements.

2.   THE FORWARD PROBLEM: BASIC EQUATIONS

From work already published[5] it is possible to numerically evalu-
ate the forward problem, where flaw shape and probe field distributions
are known. In this section we present means of simplifying the prob-
lem. Our aim is to find an approximate analytical model which predicts
ΔZ for a flaw of arbitrary dimensions in an arbitrary probe field, and
which can be parameterized to fit experimental measurements.

The crack geometry we consider is shown in Fig. 2. We choose
this particular geometry because it permits an analytic solution for
flaw interaction with nonuniform probe fields.

Although this flaw shape is not very realistic, we will show that
the results obtained are similar to "smooth", i.e., semicircular flaws
with the same aspect ratio. We conclude from this that particulars of
flaw shape have limited impact on inversion results when only the
general dimensions of the flaw are needed, as is the case for most NDE
applications. The assumption of constant opening Δu from the mouth
to the bottom of the flaw in Fig. 2 may be removed if desired.

We begin with the ΔZ formula[5]

$$\Delta Z = \frac{1}{I^2} \int_{\substack{\text{flaw} \\ \text{mouth}}} (E \times H' - E' \times H) \cdot \hat{n} \, dxdy \qquad (1)$$

TEST SURFACE

FLAW INTERIOR

Δu

a

2c

x

y

z
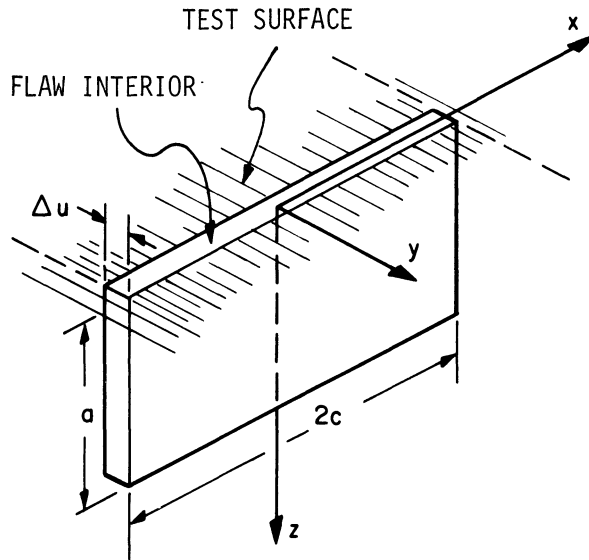
Fig. 2.   Flaw geometry.

which, in the geometry of Fig. 2, becomes

$$\Delta Z = \frac{1}{I^2} \int_{\substack{\text{flaw} \\ \text{mouth}}} (E_y H'_x - E'_y H'_x) dxdy \quad . \tag{2}$$

Note that here the outward normal, $\hat{n}$, is equal to $-\hat{z}$.

Previous work described a method of predicting ΔZ for a crack
of arbitrary length, opening, and depth, but with a uniform field
probe.   In this case, solutions can be obtained by using a large a/δ
analysis of probe-flaw interactions developed by Collins and Michael[8]
for the potential difference method of flaw detection.   This approach
cannot, however, be applied to the nonuniform field case without con-
siderable modification.   The calculations presented here are based on
a Born approximation, which assumes that the tangential magnetic field
applied by the probe to the surface of the unflawed work piece is
essentially unchanged by the presence of the flaw.   The magnetic field
inside the flaw is evaluated from the probe field applied to the mouth

of the flaw (Fig. 2) and this field can be used in evaluating the ΔZ formula, Eq. (2).

Since air has no current sources, we can represent the magnetic field by a magnetic scalar potential Ψ, which satisfies Laplace's equation, and a boundary condition that its normal derivative be zero at all metal surfaces. (The latter boundary condition is modified somewhat when we take into account the finite conductivity of the metallic surface, but holds when the crack depth is much larger than an electromagnetic skin depth.) It is true for all fatigue cracks, and for most machined notches, that the opening Δu will be much smaller than any probe dimension. This implies that inside the flaw, H must be very nearly parallel to both flaw faces (a boundary condition at the surface of a good conductor), so that Ψ is independent of the y-position within the flaw. Since this makes the y-derivative zero, we find that Ψ satisfies a two-dimensional Laplace equation inside the flaw. For the rectangular geometry, any solution of these equations (two-dimensional Laplace equation and zero normal derivative at the bottom and sides) can be expanded as a series of separated variable solutions. That is,

$$\Psi(x,z) = \sum_{n=1,3,5...}^{\infty} B_n \frac{\cosh n\pi(z-a)/(2c)}{n \cosh n\pi a/(2c)} \sin \frac{n\pi x}{2c}$$

$$+ \sum_{n=2,4,6...}^{\infty} B_n \frac{\cosh n\pi(z-a)/(2c)}{n \cosh n\pi a/(2c)} \cos \frac{n\pi x}{2c} \qquad (3)$$

where the B_n's are to be evaluated from the nonlinear probe field applied to the mouth of the flaw.

3.   FORWARD PROBLEM: COMPUTATION

From Eq. (3), we can identify the following components of E and H inside the flaw,

$$H'_x = -\frac{\partial \Psi}{\partial x}$$

$$E'_z = Z_s \frac{\partial \Psi}{\partial x} \qquad (4)$$

where the surface impedance Z_s is given by

$$Z_s = \frac{1 + i}{\sigma \delta} \qquad . \qquad (5)$$

The first term under the integral of Eq. (2) represents the surface impedance lost to the crack mouth opening. In any real crack geometry this is small compared to the wall impedance of the flaw sides.[5] The second term contains the dominant part of the eddy current response. Since we solve for the magnetic potential inside the flaw, H_x' is available for direct computation, but not E_x'. We must therefore manipulate the second part of Eq. (2) to eliminate E_x'. Performing the y-integration first, and using the integral form of Faraday's law, we obtain:

$$-\int_{-\Delta u/2}^{\Delta u/2} E_y' d\dot{y} + 2 \int_0^a E_z' d\dot{z} = i\omega\mu_0 \int_{\substack{flaw \\ section}} H_x' d\dot{y}dz \quad ; \qquad (6)$$

then

$$\int E_y' d\dot{y} = (i\omega\Delta u + 2Z_s) \int_0^a \frac{\partial\Psi}{\partial x} \, dz \quad ,$$

from which we can write an expression for ΔZ depending only on Ψ,

$$\Delta Z = \frac{1}{I^2\sigma} \left\{ -\frac{1+i}{\delta} \int_{\substack{flaw \\ mouth}} \left(\frac{\partial\Psi}{\partial x}\right)^2_{z=0} dxdy \right.$$

$$\left. + \left(i\frac{2\Delta u}{\delta^2} + 2\frac{1+i}{\delta}\right)\iint dx\left[\left(\frac{\partial\Psi}{\partial z}\right)_{z=0} \int_0^a dz\frac{\partial\Psi}{\partial x}\right]\right\} \quad (7)$$

Since the magnetic field does not vary significantly over the relatively small width of the crack, it is possible to replace the "flaw mouth" integral with

$$\int_{-c}^{+c} \left(\frac{\partial\Psi}{\partial x}\right)^2_{z=0} \Delta u dy \quad .$$

For the rectangular crack geometry, there are three regions requiring "local" corner correction: the lips, the sides, and the bottom (or tip) of the crack. Since the sides are geometrically crack tip structures, like the bottom, the correction is physically the same and it is convenient to lump these two corrections together as ΔZ_t. The lip correction is called ΔZ_ℓ. These two corrections

are given by

$$\Delta Z_t = \frac{k_t}{I^2 \sigma} \int_{-c}^{+c} dx \left(\frac{\partial \Psi}{\partial x}\right)^2_{z=a} + \int_0^a dz \left(\frac{\partial \Psi}{\partial z}\right)_{x=\pm c}$$

(8)

$$\Delta Z_\ell = \frac{k_\ell}{I^2 \sigma} \int_{-c}^{+c} dx \left(\frac{\partial \Psi}{\partial x}\right)^2_{z=0} \quad .$$

In the above, $k_t = 1.0$, and $k_\ell = -2.56$ are constants obtained from Kahn's[9] numerical work for a two-dimensional crack in a uniform field, on the assumption that the fields at the lips and tips of the crack behave locally as in the two-dimensional problem (large a/δ).

Inserting the expression for Ψ from Eq. (3), we find that

$$\Delta Z = 2 \frac{c}{\delta} \left\{ \Sigma^0 + (1+i) \frac{c}{\delta} \Sigma^1 + \frac{i\Delta uc}{\delta^2} \Sigma^2 \right\}$$

(9)

where the coefficients are given by

$$\Sigma^0 = \frac{a}{c} k_t \left[\frac{\pi^2}{16} \sum_n B_n^2 \frac{2 - \frac{a}{c} + \frac{1}{n\pi} \sinh(n\pi a/c)}{(\cosh n\pi a/(2c))^2} \right.$$

$$+ \frac{\pi}{2} \sum_{n \neq m} \frac{|B_n B_m|}{\cosh(m\pi a/c)\cosh n\pi a/(2c)} \left(\frac{\sinh(m+n)\frac{\pi a}{2c}}{m+n} - \frac{\sinh(m-n)\frac{\pi a}{2c}}{m-n} \right) \Bigg]$$

$$+ k_\ell \frac{\pi^2 a}{8c} \sum_n B_n^2 \quad ,$$

$$\Sigma^1 = \frac{\pi}{2} \sum_n B_n^2 \frac{(\tanh \frac{n\pi a}{2c})^2}{n} \quad .$$

(10)

Although the algebraic details of Eq. (9) are dependent on the geometry chosen, the general form is expected to remain the same for any crack shape .in the large a/δ regime. The three terms correspond roughly to resistive losses at the crack corners, wall impedance of current flowing over the flaw surfaces, and Faraday induction due to the volume enclosed by currents encircling the flaw. More detailed modeling should result in changes to the values of the Σ's , but that is all.

4.   COMPUTATION OF Ψ_I

Solving for Ψ_I in the entire region including the flaw and the probe is very involved. This would *not* give us a simple mathematical model easily parameterized for inversion purposes. Instead, as we noted above, we make a Born approximation; that is, we simply demand that the interior solution Ψ_I match the probe potential Ψ_{probe} at the flaw mouth. Physically, this amounts to equating the tangential components of the interior field and the probe field at the flaw mouth. The result is that the B_n's from Eq. (3) become

$$B_n = \frac{n}{c^2 H_0} \int_{-c}^{c} \Psi_0 \; \text{cir} \; \frac{n\pi x}{2c} \; dx \quad . \tag{11}$$

Here H_0 is a factor relating the phase and amplitude of the probe field on the work surface to Eq. (1) and "cir" is a trigonometric function given by

$$\text{cir} \; \frac{n\pi x}{2c} = \begin{cases} \sin \dfrac{n\pi x}{2c} \quad , \quad \text{if} \quad n \quad \text{odd}; \\ \\ \cos \dfrac{n\pi x}{2c} \quad , \quad \text{if} \quad n \quad \text{even} \; . \end{cases} \tag{12}$$

The B_n's depend on the crack length $2c$, and on the probe field Ψ_0, but not on the crack depth a. With this expression for Ψ, we can now evaluate the Σ's of Eq. (9). These are plotted against a/c in Fig. 3 for both a uniform and linearly varying probe field at the flaw mouth (corresponding to linearly and quadratically varying Ψ in Eq. (11)).

5.   PARAMETERIZATION OF Ψ

In inversion, we do not want to recalculate the B's (through Eq. (11)) for each crack size and probe field geometry, so we express the potential at the unflawed work surface as the truncated Taylor expansion

$$\Psi_{probe}(x + x_0) = \Psi(x_0) + x h_0 + \frac{x^2}{2} h_1 \tag{13}$$

where the h_0 is the strength of the probe field at x_0 and h_1 is its first derivative. These two coefficients are implicitly functions of the global position x_0 of the crack with respect to the probe field, and govern the flaw response, since the constant term integrates to zero in Eq. (11). Note that the origin of the coordinate x is attached to the probe and x_0 is the probe position in this coordinate system.
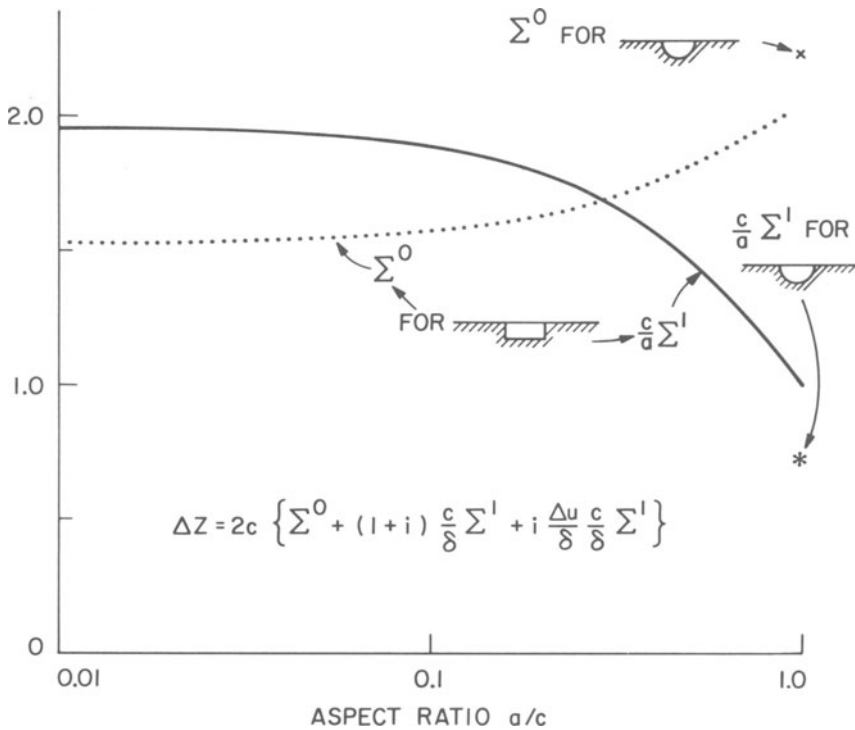
Fig. 3. Σ Coefficients for uniform field.

Since the even and odd B_n's are integrals with even and odd weighting functions, the first term in Eq. (13) will not contribute to the even B_n's , and the second term will not contribute to the odd B_n's . The summation terms (Eq. (10)) in Fig. 3 all involve squares of B_n's or products of B_n's with the same parity and therefore have the same dependence on h_0 or h_1 . If Ψ_{probe} can be adequately described by Eq. (13), the Σ's become

$$\Sigma^0 = \Sigma_0^0 h_0^2 + \Sigma_1^0 c^2 h_1^2$$

$$(14)$$

$$\Sigma^1 = \Sigma_0^1 h_0^2 + \Sigma_1^1 c^2 h_1^2$$

where Σ_0^0 is Σ^0 calculated for $\Psi_{probe} = x$, with $c = 1$ and Σ_1^0 is Σ^0 calculated for $\Psi_{probe} = x$, with $c = 1$. The Σ^1 coefficients are similarly defined. These coefficients are, of course, exactly those plotted in Fig. 3. (Note that the subscripts and superscripts are not intended to indicate matrix elements!) For the

rectangular crack geometry considered, $\Sigma^1 = \Sigma^2$ in Eq. (9); we there-
fore use Σ^1 throughout, in developing our inversion protocol. It
should be remembered, however, that there may be a correction factor
in the last term of Eq. (9).

For comparison, in Fig. 3 we have indicated the values of Σ^0
and Σ^1 calculated for a uniform field probe and semicircular crack.[5]
Although these values are somewhat different, they justify our asser-
tion that the results are not highly shape sensitive. Furthermore,
the prediction of the simplified theory presented here may be adjusted
empirically according to experimental experience, or "exact" values of
the Σ's determined by numerical analysis (e.g., finite element[10] or
integral equation[11] methods) may be inserted.

6.   INVERSION, "UNIFORM" FIELD

We consider first the simplest inversion case, where the field is
uniform, and well-determined. From Eq. (9),

$$\Delta Z = 2c\Sigma_0^0 + \frac{2c^2}{\delta}\Sigma_0^1 + \frac{2\Delta uc^2}{\delta^2}\Sigma_0^1 \quad . \tag{15}$$

In this equation, the only dependence on frequency is through the skin
depth δ. By making three measurements at different frequencies
(i.e., three different values of δ), we obtain three equations from
which we can determine the coefficients $c\Sigma_0^0$, $c^2\Sigma_0^1$, and $\Delta uc^2\Sigma_0^1$.
Dividing the last two coefficients gives Δu directly, and taking the
quotient $c^2\Sigma_0^1/(c\Sigma_0^0)^2$, gives a function that depends on a/c only.
This uniquely determines a/c, from which we can calculate a value
for Σ_0^1, and hence c.

The above procedure suffers from several serious disadvantages.
Since the model is not exact, one cannot expect three measurements to
consistently predict the flaw dimensions. Some optimum filtering is
required. Also, there will be noise in the three measurements, making
it necessary to average over many measurements. Both the above diffi-
culties can be dealt with by making measurements over a range of fre-
quencies, and then using a least squares technique to find a best fit
of Eq. (9) to these data. We could further improve the technique by
using nonlinear least squares techniques (such as a Levenberg-
Marquadart algorithm) to fit values of a, c, and Δu directly to
the data.

7.   INVERSION: NONUNIFORM FIELD; THE REGISTRATION PROBLEM

To effect a least squares optimization we adopt the expansion of
Eq. (13), and use it in Eq. (9), giving

$$\Delta Z = 2c \left\{ \Sigma_0^0 h_0^2 + \Sigma_1^0 h_1^2 + (1+i) \frac{c}{\delta} [\Sigma_0^1 h_0^2 + \Sigma_1^1 h_1^2] + \frac{i\Delta uc}{\delta^2} [\Sigma_0^1 h_0^2 + \Sigma_1^1 h_1^2] \right\} .$$

$$(16)$$

Since the field coefficients h_0 and h_1 are functions of the un-
known flaw position relative to the probe we must address the regis-
tration problem at the same time as the inversion problem.

In Eq. (16), $h_0(x_0,y_0)$ and $h_1(x,y_0)$, expressed now in terms
of two-dimensional space variations, are the only position-dependent
parameters. It should be recalled, however, that although we expand
the probe field *locally* in a Taylor series, the coefficients are
functions of the *global* position of the flaw relative to the probe.
Thus, we write

$$\Delta Z = \zeta_0 h_0^2(x,y) + \zeta_1 h_1^2(x,y) .$$

$$(17)$$

Here, the ζ's

$$\zeta_{0/1} = 2c \left\{ \Sigma_{0/1}^0 + (1+i) \frac{c}{\delta} \Sigma_{0/1}^1 + \frac{i\Delta uc}{\delta^2} \Sigma_{0/1}^2 \right\}$$

$$(18)$$

contain all the flaw-dependent information, while the h's contain
all the field and position dependence. The goal is to find the correct
offset for the flaw position (x_0,y_0) , and the values of the ζ's
which best fit our model.

A special case exists when the ratio a/δ is much smaller than
one. In this case, the above analysis of the forward problem is not
valid. Kincaid[2] has derived for this case

$$\Delta Z = \sigma\delta \left(\frac{H_0}{I} \right)^2 z_s^2 \frac{4ac}{3} \left\{ \frac{a}{\delta} - \frac{5}{8} \frac{a^2}{\delta^2} - i \left[\frac{5}{8} \frac{a^2}{\delta^2} - \frac{4}{15} \frac{a^3}{\delta^3} \right] \right\} .$$

Clearly, this formula can be used in the same was as Eq. (9) for
inversion purposes.

8.   REGISTRATION

The signal registration problem for eddy current signals is very
similar to the problem of optical image registration, dealt with exten-
sively in the pattern recognition and aerial photography literature.
Eddy current multiposition data correspond to the "subimage" of image-

registration parlance, and the expected response $\zeta_0 h_0^2 + \zeta_1 h_1^2$ corre-
sponds to the known "image". There are, however, several differences:

(1) In eddy current registration, the "image" contains two
     unknowns.

(2) Eddy current data are not always taken on a regular grid
     of points.

(3) Features tend to be larger and there are no detailed
     features (cities, rivers, etc.) to lock on to.

The registration algorithm which seems most useful in eddy
current applications is that proposed by Barnea and Silverman,[12]
henceforth referred to as SSDA (Sequential Similarity Detection
Algorithm). This method has several inherent advantages:

(1) It allows very flexible means of dealing with noise, and
     performs well in high-noise situations.

(2) Data need not be taken at regular intervals.

(3) *A priori* information (aspect ratio, expected distribution,
     etc.) can be used in a natural way to speed computation
     and improve accuracy.

(4) Optimization of the image (i.e., determination of the ζ's)
     can be incorporated into the registration process.

The only modification of the SSDA technique needed in applying
it to the eddy current problem is to replace the error function
(Eqs. (7) and (11) in reference 12)

$$E(i,j) \;\; = \;\; \sum_{\substack{\ell=1 \\ m=1}}^{M} \left| S_M^{i,j}(\ell,m) - W(\ell,m) \right|$$

with a least squares error function

$$E = \min_{\zeta_0, \zeta_1} \sum_{m=1}^{N} \left| \zeta_0 h_0^2(x_m - x_0, y_m - y_0) + \zeta_1 h_1^2(x_m - x_0, y_m - y_0) - \Delta z_m \right|^2 \; .$$

$$(19)$$

Here, there are N observations of ΔZ , labeled ΔZ_m . The pair
(x_m, y_m) is the (known) position of the probe in the work piece during
observation m . We assume that the functions $h_0(x,y)^2$ and $h_1(x,y)^2$
are known from experiment or theoretical prediction. (Note that both
the x_m and x_0 coordinates are *now* referenced to a point on the work

piece.) In Eq. (13) the origin of x was attached to the probe.
The algorithm works in the same manner as before, testing tentative
registrations until an error threshold is exceeded. Only the means
of error evaluation is changed.

In operation, calculating the minimum in Eq. (19) is easier than
it might seem. When the nth sample is taken from a trial registra-
tion, minimization requires the solution of the linear equations

$$\zeta_0 \sum_m h_0^4 + \zeta_1 \sum_m h_0^2 h_1^2 = \sum_m \Delta z_m h_0^2$$

$$\zeta_0 \sum_m h_0^2 h_1^2 + \zeta_1 \sum_m h_1^4 = \sum_m \Delta z_m h_1^2$$

$$(20)$$

where all summations are over the number of observations, and the h's
are evaluated at the points $(x_m - x_0, y_m - y_0)$. The least squares
error is then given by

$$E = \sum_m \Delta z_m^2 + \zeta_0^2 \sum_m h_0^4 + \zeta_1^2 \sum_m h_1^4$$
$$- 2\zeta_0 \sum_m \Delta z_m h_0^2 - 2\zeta_0 \sum_m \Delta z_m h_0^2 \qquad (21)$$
$$+ 2\zeta_0 \zeta_1 \sum_m h_0^2 h_1^2 \quad .$$

Computationally, the six sums are initialized when the algorithm
begins evaluating a new trial registration, and are simply updated
each time the error does not exceed threshold.

In most situations, it will be desirable to include measurements
at different frequencies as well as positions into the registration
procedure, rather than registering on data taken at one frequency and
performing inversion as a separate step. This is in order to expand
the data base (and reduce susceptibility to noise) on which our regis-
tration depends. In this case, the ζ's will no longer be indepen-
dent of frequency, but must be written out in the polynomial form of
Eq. (16):

$$E = \min_{\substack{v_0, v_1, v_2 \\ v_0', v_1', v_2'}} \sum_S \left[\left(v_0 + \frac{v_1}{\delta_j} + \frac{v_2}{\delta_j^2} \right) h_0^2 (x_m - x_0, y_m - y_0) \right.$$
$$\left. \left(v_0' + \frac{v_1'}{\delta_j} + \frac{v_2'}{\delta_j^2} \right) h_1^2 (x_m - x_0, y_m - y_0) - \Delta z_{m,j} \right]^2 \qquad (22)$$

where the summation set S represents all frequencies ω_j and positions (x_m, y_m) for $m = 1$ to n; the v's are the coefficients of Eq. (16). Although this will still result in a linear equation for minimization, the solution matrix will have much higher dimensionality. Another danger is that the number of minimization parameters $(v_0, v_1, v_2, v_0', v_1', v_2' = 6)$ is larger than the number of physical variables $(a, c, \Delta u = 3)$. Thus, it may be advantageous to perform a separate registration for each frequency, and take a weighted average of the results. Yet another consideration may be that h_0 and h_1 could depend on frequency. This will occur if a probe has a field whose global distribution depends on frequency, or if we must use different probes at different frequencies.

9. "LIFTOFF" CONSIDERATIONS

In the above discussion, it was assumed that one could measure both components (real and imaginary) of ΔZ. In actual testing situations, there will be some degree of "liftoff" noise, and some measures must be foreseen to counteract this. A very common approach to this problem is to rotate the output of the eddy current instrument so that the "liftoff" signal is (to first order) parallel to the horizontal channel. One then takes the *vertical* channel as a liftoff-free output.[3]

We can insert this into Eq. (9) by taking only the component of each of the terms in the "quadrature" direction (the direction perpendicular to "liftoff"). Although this is very simple conceptually, there are some subtleties. The three Σ's are real numbers, so that the projection can be performed by substituting appropriate trigonometric functions for the phase factors in front of each term. Since the "liftoff" direction is known, this does not add any unknowns to the inversion procedure.

10. EXPERIMENTAL GOALS

The previous portion of our paper proposes an inversion protocol for inverting multiposition, multifrequency data to obtain overall flaw dimensions. To do this effectively, we need to be able to make measurements over a broad range of frequencies with a single probe.

One goal of the experimental effort was to test the accuracy of the theory on which our inversion procedure depends, since inversion based on an inaccurate model of the flaw response is doomed to failure. It was decided that the only way to obtain test samples with known flaw dimensions would be to scale the flaws up.[2] The samples, machined and electric discharge machined (EDM) slots in aluminum and stainless steel, had depts ranging from 0.5 mm to 5.0 mm.

For optimum detection, a range of a/δ between one and one hundred appears to be most favorable.[2,3,4] Note that this range in δ corresponds to a range in frequency of four decades. The probe was designed to be operable at least over the 100 kHz — 10 MHz frequency range. Actual measurements were taken from 100 kHz to 10 MHz. This gives a range of 1.4 to 250 in a/δ for the aluminum samples and 0.4 to 25 for the stainless steel samples.

11. THE BROADBAND PROBE

Construction of the broadband probe and bridge assembly was guided by the following principles:

(1) There is no internal bridge-nulling circuitry. If the probe is to be truly broadband instrument, we do not want to change bridge parameters when we step from one frequency to another.

(2) The bridge contains two fixed probe coils with access to the work piece, much like standard differential eddy current probes. This is a necessity for operation on materials of different conductivities.

(3) The differential probes are widely separated in space, so that the external fields of both can be calculated in a straightforward manner and they can each interact separately with a flaw.

(4) All components must be capable of broadband operation.

The heart of the broadband probe, illustrated in Fig. 4, is a high frequency four-port hybrid, which acts as a Wheatstone bridge. For operation at the frequencies of interest, the hybrid is realized as seven ferrite core precision-wound transformers. Transformers T5 and T6 correspond to the two upper arms of the usual Wheatstone bridge, transformer pairs T1, T2, and T3, T4 step up the impedance of the probe coils L1 and L2, increasing signal output, and transformer T7 converts the bipolar imbalance signal to the unipolar output Δ. This entire assembly mounts in an enclosure approximately 30 mm by 30 mm by 50 mm, with the two probes in a coplanar configuration on one side of the enclosure.

For all measurements, a 1 V (peak-to-peak) signal is applied to the Σ-port of the probe and measurements are taken at the Δ-port. To observe the phase of Δ relative to Σ, a dual-trace oscilloscope was used for measurements in the 100 kHz to 2 MHz range, and a commercially made phase-gain meter in the 1 MHz to 25 MHz range. The
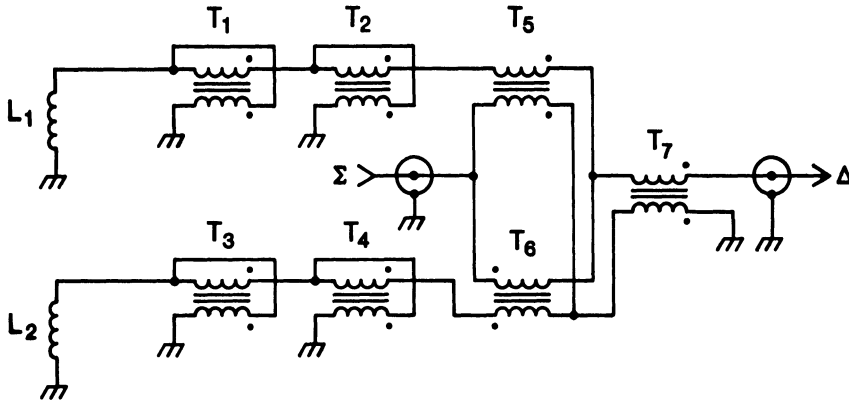
Fig. 4. Broadband eddy current bridge-probe configuration.

1 MHz overlap region allows comparison of the two methods. At 1 MHz, the voltage level at the output port (Σ) in the absence of any flaw and for balanced (25 μm) "liftoff" distance at the two probes (L1 and L2) was approximately 2 mV. At 20 MHz, this background signal (caused by the bridge being out of balance) was 4.4 mV. This is a measure of the good common mode rejection (CMR) achieved.

12. MEASUREMENT PROCEDURE

One of our guiding principles stated above is that we do not want to "null" the probe internally for each measurement. This means that we must subtract the inherent bridge imbalance (background) signal which may be due to the limitations of the construction techniques. When we measure a vector voltage at the Δ port of the probe, what we are really measuring is a vector sum, $\Delta V_U + \Delta V_F$, of the flaw voltage and the imbalance voltage. Since the voltages are small compared with the bridge drive voltage, they are related to changes in probe impedance by the same proportionality constant (K in Fig. 5). To retrieve the flaw signal, however, it is necessary to vectorially subtract the background unbalance voltage. The procedure is illustrated in Fig. 5.

We first measure the imbalance signal ΔV_U by moving the probe off-crack. The on-flaw measurement, when subtracted in the manner described above, gives us the desired signal ΔV_F . Evaluating the "liftoff" (or tilt) signal proceeds in a similar manner. We vectorially subtract the non-"liftoff" signal from the measured "liftoff" signal.

13. RESULTS

The first experiments with the new eddy current probe were conducted on a tightly closed fatigue crack in an aluminum tension specimen. Figures 6 and 7 depict the results when we scan the probe across
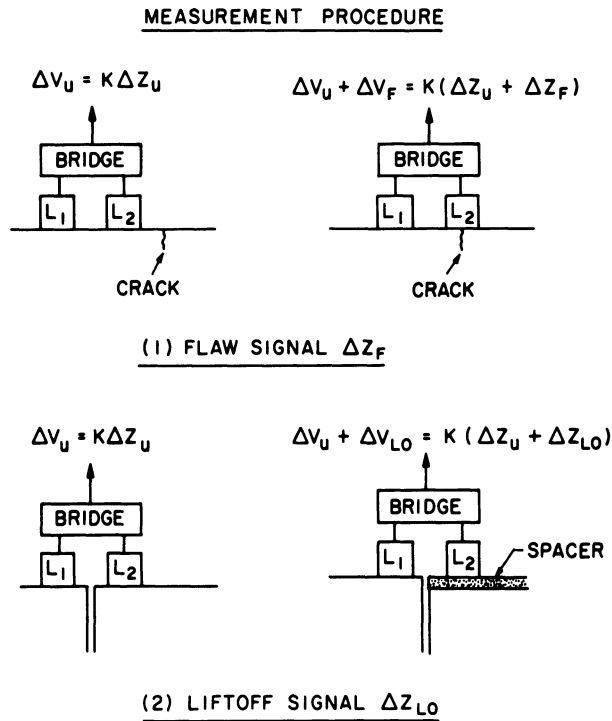
MEASUREMENT PROCEDURE

$$\Delta V_u = K \Delta Z_u \qquad\qquad \Delta V_u + \Delta V_F = K(\Delta Z_u + \Delta Z_F)$$

BRIDGE

L_1 L_2

CRACK

BRIDGE

L_1 L_2

CRACK

(1) FLAW SIGNAL ΔZ_F

$$\Delta V_u = K \Delta Z_u \qquad\qquad \Delta V_u + \Delta V_{LO} = K(\Delta Z_u + \Delta Z_{LO})$$

BRIDGE

L_1 L_2

BRIDGE

L_1 L_2 — SPACER

(2) LIFTOFF SIGNAL ΔZ_{LO}

Fig. 5. Two measurements are necessary to separate a desired voltage from imbalance signal.

the short dimension of the crack. This crack was approximately 5 mm long and 2 mm deep. In these figures, the signal is plotted as a function of probe position along the scan line. Measurements were taken at 200 kHz, 500 kHz, 1 MHz, 5 MHz, 10 MHz, and 20 MHz. As can be seen in Fig. 6 , the phase excursion first becomes positive and then negative in relation to the phase of the background (bridge imbalance) signal. The maximum positive excursion corresponds to the coincidence of the "in-phase" probe with the center of the crack, and the maximum negative excursion corresponds to the coincidence of the "out-of-phase" probe with the center of the crack. The spacing of the two probes ($L1$ and $L2$) was approximately 33 mm.
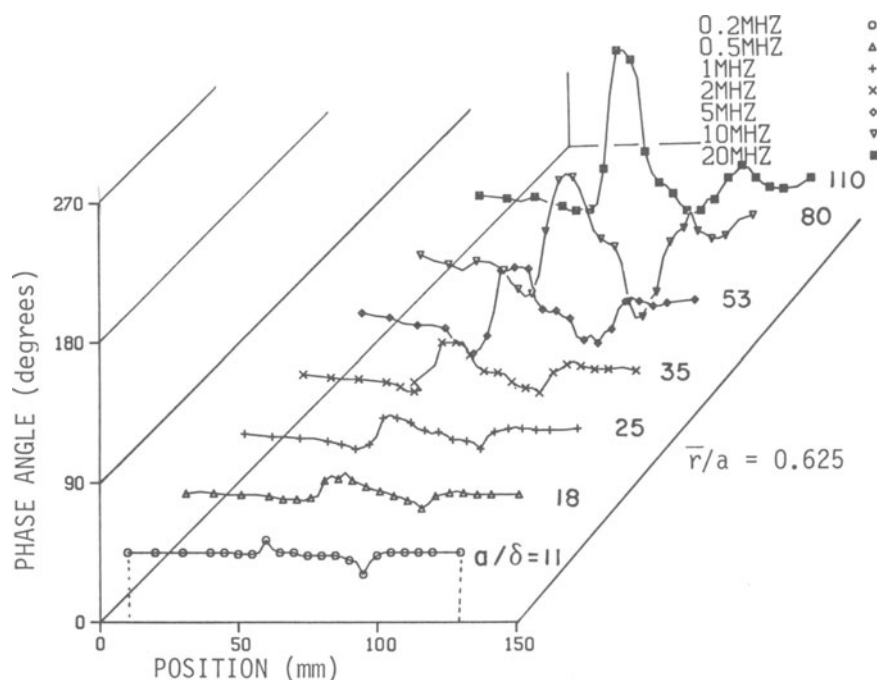
Fig. 6. Probe signal phase (uncorrected for imbalance).

Comparing this with Fig. 7, it appears that amplitude is much less sensitive than phase in detecting cracks, especially at lower frequencies. This is not necessarily true. Since the imbalance signal adds vectorially to the flaw signal, it may happen that the flaw signal is perpendicular, so that the resultant vector will change phase but not amplitude.

The most striking feature of Figs. 6 and 7 is that the response increases dramatically in both phase and amplitude as frequency increases. This is consistent with the theoretical prediction that flaw response should be proportional to frequency,[3] and suggests that it may be advantageous for detection to operate at high frequencies.

We plot the reduced data from a series of slots in aluminum and stainless steel in Fig. 8. Note that the horizontal axis in this figure is $\bar{r}/\delta$, where $\bar{r}$ is the diameter of the coil used (the probe described here has a spiral structure, with average diameter of 1.25 mm). The first plot of the figure is the theoretical prediction of Dodd and Deeds[13] for a square cross-section coil (compare with the dashed line in the third part of the figure). The second and third parts show the phase angle variation of the flaw voltage ΔV_F when the probe is positioned directly over the slot. All the slots
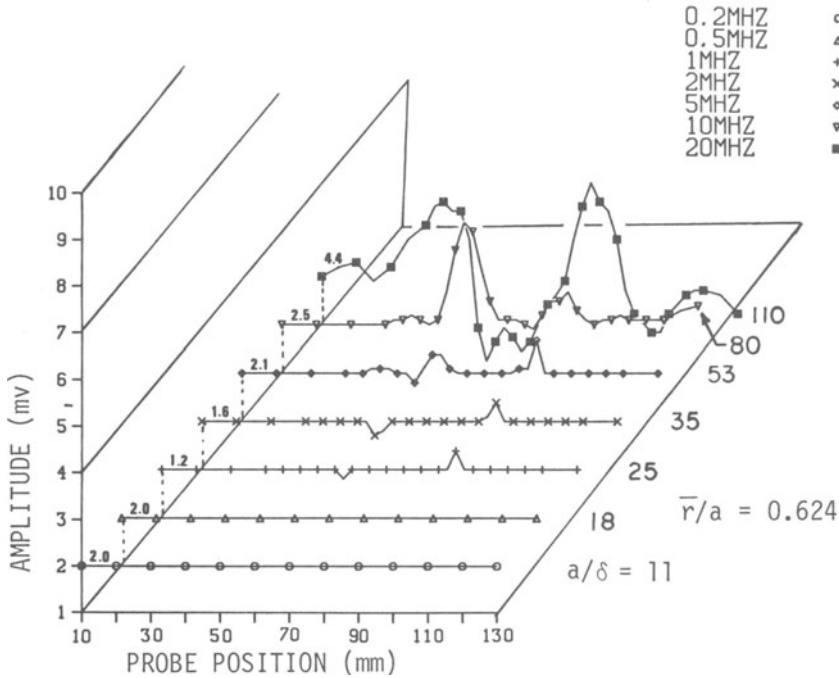
Fig. 7. Probe signal amplitude (uncorrected for imbalance).

were much longer than the probe (so that two-dimensional theory is applicable). Several features of the plots in parts two and three are in agreement with theoretical expectations, especially that the shape of the flaw responses as a function of $\bar{r}/\delta$ is very similar to the Dodd and Deeds[13] curve.

Another interesting feature of these curves is that the effects of flaw depth on relative phase saturate more quickly at high frequencies than at low frequencies — note the departure of the curves numbered 2 at low $\bar{r}/\delta$. This is in agreement with the theory presented in reference 1, and reproduced in Fig. 9. At high frequencies a/δ becomes large, so that the second and fourth terms in the curly brackets become insignificant. The remaining two terms have the same dependence on the depth a, so that changes in a do not affect the phase. At low frequencies, the second term *is* important (though not dominant), so that changes in the other terms, which have a different phase angle, produce an overall phase shift of ΔV_F.
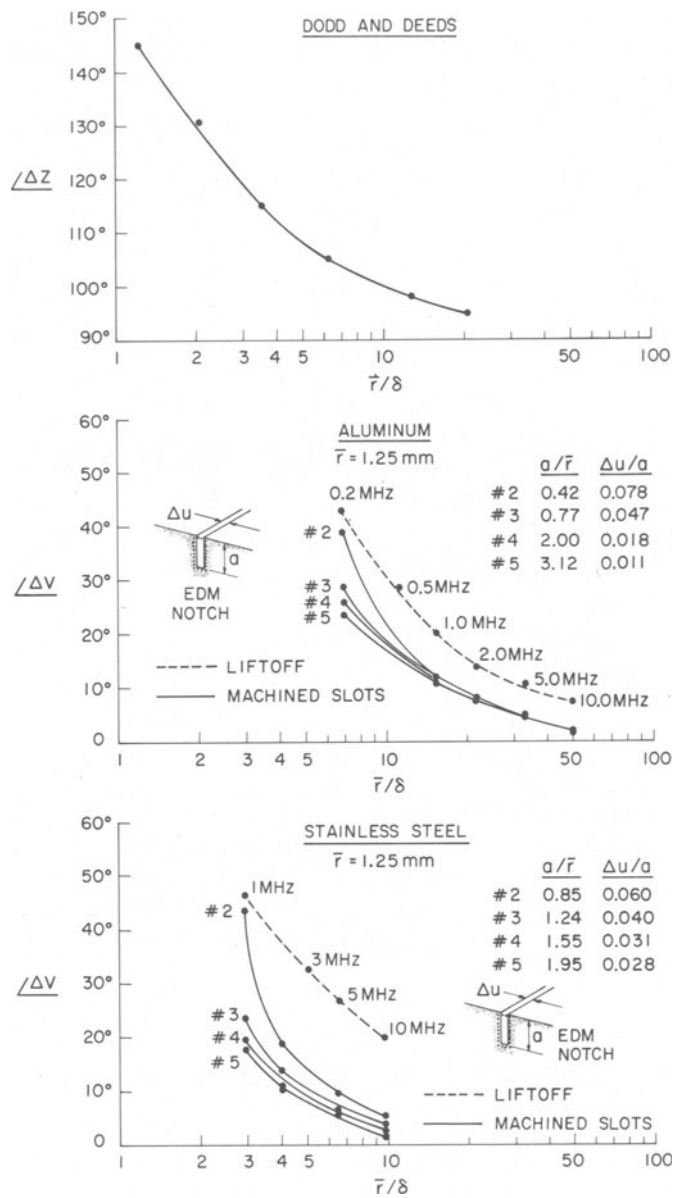
Fig. 8. *Top:* Plot of phase from reference 13. *Middle:* Normalized phase for aluminum slots. *Bottom:* Normalized phase for slots in stainless steel.

TWO-DIMENSIONAL CRACK - NONUNIFORM FIELD

LARGE a/δ; $2\pi/k \gg \delta$

CRACK RESPONSE TO FULL SPATIAL FREQUENCY SPECTRUM

$$\Delta Z_u = \frac{1}{\sigma I^2} \int_{-\infty}^{\infty} \left| h^I(k) \right|^2 \left\{ 2(1+i)\frac{a}{\delta} G(k) + (e^{-2ka} - 2.56) + i\frac{A_F}{\delta^2} G(k) - (1+i)\frac{\Delta u}{\delta} \right\} dk$$
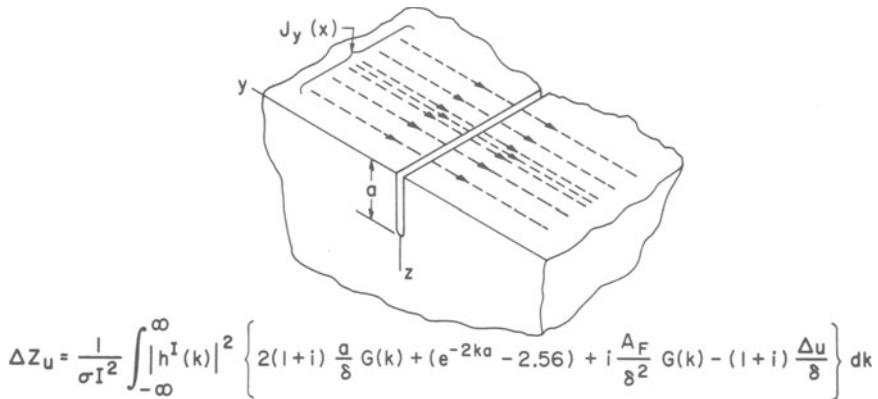
Fig. 9.   Theoretical two-dimensional nonuniform field response.
$G(k) = (1-e^{-2ka})/ka$.

14.   CONCLUSION

The forward solution which we have presented for the "rectangular" crack is the first example of a calculation which allows for arbitrary flaw dimensions as well as arbitrary probe field shape. Our inversion technique is also the first of its kind, systematically extracting the position and overall dimensions of a surface-breaking crack.

The probe we described is especially intended for the broadband (multifrequency) measurements needed for our inversion method. We further extend the range in a/δ by using slots in materials having different conductivities. The measurements we report on are still in progress, as is the reduction of the data and comparison with applicable theories. In future experiments, we intend to work with flaws which are smaller than the probe, so as to test the theories developed in this paper.

Another set of experiments we have planned involve measurement of the probe field itself. Miniature Hall-effect probes have been used in the past in connection with measurements on magnetic disk heads. This method could be used for eddy current probes as well, but it may be more effective to use the probe's own flaw response (on a flaw of

known dimensions and shape) to determine its magnetic field distribution. This has the advantage that measurements are made with the probe on the test surface, rather than in air.

REFERENCES

1. B.A. Auld, F. Muennemann, M. Riaziat, and D.K. Winslow, Analytical Methods in Eddy Current NDE, in: "Review of Progress in Quantitative NDE," D.O. Thompson and D. Chimenti, eds., University of Colorado, Boulder, August 2-7, 1981, Plenum Press, New York (1982), in press.

2. T.G. Kincaid, Probe Designs, in: "Review of Progress in Quantitative NDE," D.O. Thompson and D. Chimenti, eds., University of California, La Jolla, August 1-6, 1982, Plenum Press, New York (1982), in press.

3. M. Riaziat and B.A. Auld, Eddy Current Probe Design and Matched Filtering for Optimum Flaw Detection, in: "Review of Progress in Quantitative NDE," D.O. Thompson and D. Chimenti, eds., University of California, La Jolla, August 1-6, 1982, Plenum Press, New York (1982), in press.

4. A.J. Bahr and E.W. Cooley, Analysis and Design of Eddy Current Measurement Systems, in: "Review of Progress in Quantitative NDE," D.O. Thompson and D. Chimenti, eds., University of California, La Jolla, August 1-6, 1982, Plenum Press, New York (1982), in press.

5. B.A. Auld, F. Muennemann, and D.K. Winslow, "Eddy Current Probe Response to Open and Closed Surface Flaws," J. Nondestructive Evaluation, 2:1 (1981).

6. W.D. Dover, F.D.W. Charlesworth, K.A. Taylor, R. Collins, and D.H. Michael, "Eddy Current Characterization of Materials and Structures," G. Birnbaum and G. Free, eds., ASTM STP, Philadelphia (1981), pp. 401-427.

7. B.A. Auld, F. Muennemann, and D.K. Winslow, Surface Flaw Detection with the Ferromagnetic Resonance Probe, in: "Review of Progress in Quantitative NDE," R.B. Thompson and P.M. Beckham, eds., AFWAL-TR-81-4080 (1980).

8. D.H. Michael, R.T. Wechter, and R. Collins, "The Measurement of Surface Cracks in Metals by Using AC Electric Fields," Proc. R. Soc. Lond. A381:139 (1982).

9. A. Kahn, R. Spal, and A. Feldman, "Eddy Current Losses Due to a
    Surface Crack in Conducting Material," J. Appl. Phys. 48:4454
    (1977).

10. R. Palanisamy and K.M. Lakin, Development of an Eddy Current
    Inspection Technique for Sleeved Engine Disk Bolt Holes, in:
    "Review of Progress in Quantitative NDE," D.O. Thompson and
    D. Chimenti, eds., University of California, La Jolla,
    August 1-6, 1982, Plenum Press, New York (1982), in press.

11. H.A. Sabbagh, A Model of Eddy Current Probes with Ferrite Cores,
    in: "Review of Progress in Quantitative NDE," D.O. Thompson
    and D. Chimenti, eds., University of California, La Jolla,
    August 1-6, 1982, Plenum Press, New York (1982), in press.

12. D.I. Barnea and H.F. Silverman, "A Class of Algorithms for Fast
    Digital Image Registration," IEEE Trans. Comput. C-21:179
    (Feb. 1972).

13. C.V. Dodd and W.E. Deeds, "Analytical Solutions to Eddy-Current
    Probe-Coil Problems," J. Appl. Phys. 39:2829 (1968).

DISCUSSION

R.B. King (National Bureau of Standards): I thought the comment about
    this being a lab instrument seemed a little restrictive. I can
    think of some field geometries, such as pipelines, where the co-
    planar nature of the two probes wouldn't hurt you, so there are
    some applications where I think you could use this.

F. Muennemann (Stanford University): That's true. Also, the geom-
    etry of the two probes could be altered somewhat to suit the
    particular geometry. We're just saying that we haven't devel-
    oped it right now with the intention of making a field test
    instrument. We are intending it as a theoretical instrument,
    at least for the time being.

D.H. Michael (University College London): It is interesting that at
    the present state, you don't use the Poisson equations, as I
    understand it.

F. Muennemann: That's correct. If you wanted to make a second Born
    approximation we would, however, have to take that into account.

D.H. Michael: Yes. I was intrigued by the formulation of that equa-
    tion. The whole problem starts out as being a Helmholtz equa-
    tion. Can you say something about how it comes down to being a
    Poisson equation?

F. Muennemann: The source term is, of course, just the Z component;
    that is, the perpendicular component of the magnetic field at
    that point. If you now restrict yourself to two dimensions,
    that third component which we are assuming is unchanged will be-
    come the source term in two dimensions.

D.H. Michael: Would you start off with the Helmholtz equation?

F. Muennemann: For the case of finite skin depth?

D.H. Michael: Yes.

F. Muennemann: When you make the first order approximation to a
    very small, vanishingly small skin depth, then that becomes a
    Laplace equation.

M. Resch (Stanford University): Do you have any thoughts about the
    minimum detectable crack size of a probe geometry like this,
    and also how crack closure would affect detectability with this
    type of probe?

F. Muennemann: I don't have any direct experience using this probe,
    so I'd be hesitant to tell you.

C.M. Fortunko (National Bureau of Standards): Can you potentially
    extend the bridge construction to much higher frequency ranges?
    For example, you must increase the frequency on small cracks,
    and this bridge type can be used at 200 MHz.

F. Muennemann: Perhaps if I could briefly steer you to this equa-
    tion. This final term is a Faraday induction term, which is
    entirely due to crack opening, and is also inversely proportional
    to the square of the skin depth, which means it will be directly
    proportional to the frequency. This term will grow linearly
    with frequency if you have a crack opening present.